1-1-1995

Femtosecond Laser-Produced Plasma X-Rays from Periodically Modulated Surface Targets

J. C. Gautheir
Ecole Polytechnique

S. Bastiani
Ecole Polytechnique

P. Audebert
Ecole Polytechnique

J. P. Geindre
Ecole Polytechnique

K. Neuman
University of California - Berkeley

See next page for additional authors

Invited Paper

Femtosecond laser-produced plasma x-rays from periodically modulated surface targets

J.C. Gauthier, S. Bastiani, P. Audebert, J.P. Geindre

Laboratoire pour l'Utilisation des Lasers Intenses,
Ecole Polytechnique, 91128 Palaiseau, (France)
Tel: (33) 1 69334112, Fax: (33) 1 69333009, e-mail: gauthier@greco2.polytechnique.fr

K. Neuman, T. Donnelly, M. Hoffer, R.W. Falcone

Department of Physics, University of California at Berkeley, Berkeley, California 94720
Tel: (510) 6428916, Fax: (510) 6438497, e-mail: rwf@physics.berkeley.edu

R. Shepherd, D. Price, B. White

Lawrence Livermore National Laboratory, PO Box 808, Livermore, California 94550
Tel: (510) 4237456, Fax: (510) 423 5998, e-mail: bill_white@internetqm.llnl.gov

ABSTRACT

We have studied theoretically and experimentally the x-ray production above 1 keV from femtosecond laser plasmas generated on periodically modulated surface targets. Laser energy coupling to plasma surface waves has been modeled using a numerical differential method. Almost total absorption of incident laser radiation is predicted for optimized interaction conditions. Silicon gratings have been irradiated by a $120fs$ Ti:sapphire laser at irradiances in excess of $10^{16}W/cm^2$. X-ray intensities above 1.5 keV (K-shell lines) have been measured as a function of the incidence angle. Results show a distinct x-ray emission maximum for the first order diffraction angle and are in good qualitative agreement with our theoretical predictions.

1 INTRODUCTION

High intensity short-pulse lasers have opened up possibilities in the production of ultra short x-ray pulses (less than $2ps$ and instrument limited) from near-solid density plasmas.[1-3] The laser pulse absorption and the x-ray conversion efficiency are characterized by the laser wavelength, the pulse duration, the irradiance, the polarization, the angle of incidence and so on.[4-11] These laser parameters govern the temporal behavior and the spatial gradients of the two most important plasma quantities, the electron temperature and density. Initially, the solid target absorbs laser energy over a distance comparable to the skin depth ($\approx 100\mathring{A}$). In the heated region, the electron temperature can reach values of $100 - 1000eV$ depending on laser intensity. At these high temperatures, thermal x-rays at energies above a kilovolt are produced. Due to the strong gradient and high

 0-8194-1882-X/95/$6.00

density, rapid quenching of x-ray emission is expected by thermal conduction into the underlying cold material and by hydrodynamic expansion.[12] Besides collisional absorption, resonance and non-collisional absorption have been shown to contribute efficiently to the overall deposition of laser light. These non-linear mechanisms produce hot electrons which give rise to bremsstrahlung and $K\alpha$ radiation from the target bulk.[10,13,14] This non-thermal emission is thought also to be very short because, in principle, hot electrons are produced only during the laser pulse.

The relative importance of collisional and resonance absorption has been shown to be governed, in model calculations,[15–17] by the value of the electron density and by the shape of the electron density gradient in the absorbing region. The quantity which is usually used to characterize the spatial extent of the plasma is the scale length L defined as $[(1/n_e)dn_e/dx]^{-1}$. The scale length is usually normalized to the laser wavelength λ_0 ($L^\star = L/\lambda_0$). One way of changing the spatial region of the plasma where absorption takes place is to vary the angle of incidence and the laser polarization. Indeed, recent measurements[18] have demonstrated that the x-ray conversion efficiency and the spectral shape of the emission show distinct dependencies on laser intensity, laser polarization and angle of incidence on the target. Another efficient way of affecting the plasma scale length is the production of a preplasma either by using the amplified spontaneous emission (ASE) of the laser system[5,19] or by deliberately using a separate long laser pulse.[20] Obviously, the nature of the target material and the roughness of the target surface will also affect the amount of absorbed laser energy and the spectral range of x-ray emission and conversion efficiency. It has been recently demonstrated that the kilovolt x-rays emitted by a flat aluminum target was greatly increased by using the ASE pedestal of a $80fs$ dye laser at a fluence close to the laser melting threshold of this material.[21,10] This can be explained in terms of surface periodic structures induced by diffraction of the light by spatial modulations of the laser (or the target) profile and interference of the diffracted waves.[22] More evidently, spatially modulated targets (gratings or gold black "foam" targets) have been shown[23] to increase significantly the laser absorption and x-ray conversion efficiencies.

In this paper, we study theoretically and experimentally the interaction of a subpicosecond laser pulse with a grating target. Laser absorption on a grating target is increased with respect to the case of the flat target by two original effects. First, diffraction by the grating couples the incident laser energy into surface electromagnetic waves (surface plasmons) which propagate along the surface. Second, the target corrugation allows the excitation of longitudinal plasma waves along the expanding electron density gradient (volume plasmons), even for normal incidence, due to resonance absorption.[24] These two effects and their coupling at critical density ($n_c = m_e\omega/4\pi e^2$; ω laser frequency) will be shown to be useful to increase and optimize the laser absorption. The paper will be organized as follows. In the first part, we describe theoretically the coupling between the incident laser electromagnetic wave and surface waves. We calculate the laser absorption efficiency of a grating target using a numerical differential method.[25] In the second part, experimental results of the He-like and $K\alpha$ emission of silicon on flat and periodically modulated targets are presented and compared to the calculations.

2 THEORY OF LASER COUPLING TO SURFACE WAVES

A surface wave is an electromagnetic wave which propagates in the vicinity of the interface between two homogeneous media.[26–28] Surface waves have been extensively studied, both theoretically and experimentally, in low irradiance laser interaction experiments,[29–31] for efficient photocathode design[32] and for the modeling of optical properties of thin film multilayers.[33]

2.1 dispersion relation of surface waves in an homogeneous medium

For the calculation of the dispersion relation of surface waves propagating at the interface between two different media, we use the propagation properties of electromagnetic waves in the two media and we connect them by

boundary conditions. The incident laser wave vector being $k_0 = \omega/c$, a plane wave solution with wave vector $\vec{k}$ at frequency ω is obtained as:

$$\vec{k} \cdot \vec{k} = \epsilon(\omega) k_0^2 \tag{1}$$

where $\epsilon(\omega)$ is the complex dielectric constant. For a plane wave incident from vacuum with an angle θ with respect to the target normal Oz (Ox and Oy define the target plane), we obtain $k_x = 0$; $k_y = \alpha\sqrt{\epsilon}\, k_0$; $k_z = \beta\sqrt{\epsilon}\, k_0$ with $\alpha^2 + \beta^2 = 1$. For $\alpha = \cos\theta$ and $\beta = \sin\theta$, we recover the ordinary case of plane waves incident with an angle θ. For imaginary values of β, α is greater than 1 and we obtain an evanescent wave in the direction perpendicular to the target and a propagating wave along the target surface. The phase velocity of this wave is lower than the speed of light. For two media with complex dielectric constants ϵ_1 and ϵ_2, the component of the field with wave vector k_y is continuous at the interface and the dispersion relation of the surface wave writes:

$$k_y^2 = \frac{\epsilon_1 \epsilon_2}{\epsilon_1 + \epsilon_2} (\frac{\omega}{c})^2. \tag{2}$$

Figure 1 shows the variation of the frequency of the surface wave as a function of the wave vector along the

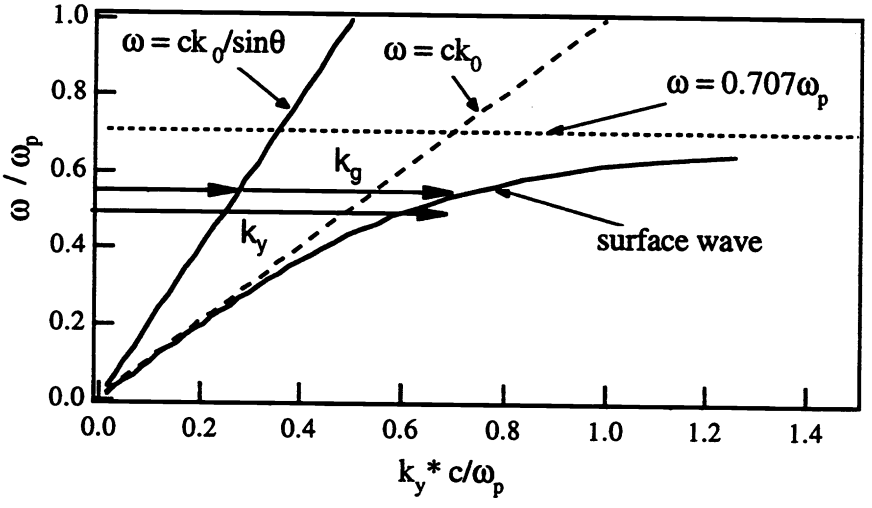

Figure 1: Dispersion relation of surface waves.

surface in the case of a wave incident upon an overcritical plasma of dielectric constant $\epsilon_2 = 1 - n_e/n_c$ (no collisions are assumed and $\epsilon_1 = 1$). We see that to couple a transverse electromagnetic wave of frequency ω, incident at an angle θ with respect to the target normal, with a surface wave of the same frequency, one has to provide an external wave vector k_g to bridge the gap between the free space wave vector $k_0/\sin\theta$ and the surface wave vector k_y. This additional wave vector can be provided by the natural (or induced) roughness of the target or by a grating with a groove spacing of $2\pi/k_g$.

The field distribution of a surface wave propagating at the interface of an overcritical plasma is shown schematically in Figure 2. To summarize, surface plasma waves have the following characteristics: i) a phase velocity lower than the speed of light, ii) an electric field distribution with a component normal or quasi-normal to the surface, iii) an inversion in the direction of the field at the interface because of the presence of oscillating charge layers, and iv) a penetrating electric field in the overcritical plasma.

Collisional damping of surface waves can be treated using the Drude model formalism for the plasma dielectric constant $\epsilon(\omega) = 1 - n_e^*/(1 + i\nu^*)$ where $n_e^* = n_e/n_c$ and $\nu^* = \nu/\omega$. For $n_e^* >> 1$ and $\nu^* < 1$, the k_y wave vector can be written, to first order (see Eq.1):

$$\frac{k_y}{k_o} \approx 1 - \frac{1}{2n_e^*}(1 - i\nu^*) \tag{3}$$

The real part of k_y is slightly smaller than k_0 and is collision frequency independent. The spatial damping of the surface wave in the y direction is governed by the imaginary part of k_y. For a constant collision frequency, the attenuation of the surface wave is lower for high electron densities.

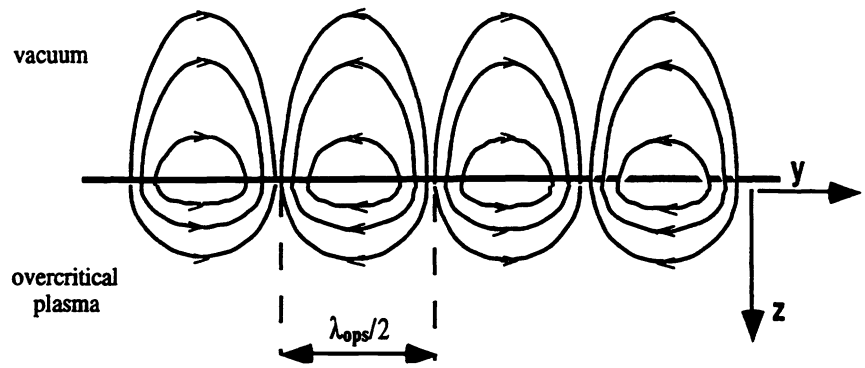

Figure 2: Schematic view of the field pattern along the interface between vacuum and an overcritical plasma.

2.2 Surface waves in a finite gradient scale length

In the general case, the interface between the two media is not perfectly steep. Then, one expects a strong coupling between the surface plasmon waves and longitudinal volume plasmon waves generated by resonance absorption at or near critical density. The dispersion relation characterizing such coupling can been obtained numerically. The Maxwell equation for the magnetic field which is parallel to the surface can be written:

$$\frac{d^2\vec{B}}{dz^2} - \frac{1}{\epsilon}\frac{d\epsilon}{dz}\frac{d\vec{B}}{dz} + \frac{\omega_0^2}{c^2}\left(\epsilon - \frac{k_y^2}{k_0^2}\right)\vec{B} = 0 \tag{4}$$

This equation is formally similar to the one describing the propagation of a plane p-polarized wave in oblique incidence. However, k_y is not constrained to be smaller than k_0 and is not even real. This equation has been solved by the Runge-Kutta method assuming a homogeneous overcritical plasma (the bulk of the target) followed by an exponential plasma density gradient. For each value of the frequency ω, we seeked a numerical value of k_y by using the following procedure: i) we initialize the calculation deep into the homogeneous plasma region by using the evanescent solution as a boundary condition, and ii) we integrate the equation across the entire electron density gradient. When the numerical solution obtained at the border of the gradient is identical to the analytical evanescent solution in vacuum we keep the trial value of k_y. Otherwise, the entire procedure is repeated with a new value of k_y. We have studied the case of exponential gradients separating vacuum (from which the laser is incident) and a $100n_c$ homogeneous plasma simulating the bulk of the target. As an approximation, the collision frequency was assumed to vary linearly with the electron density ($\nu^* = 0.01n_e^*$). Results are given in Figure 3 for a laser wavelength of $600nm$. The real part of k_y departs significantly from k_0 for large gradient scale lengths. The imaginary part of k_y gives the damping of the surface wave in the direction parallel to the surface. For gradient scale lengths larger than $20nm$, the surface wave is fully damped. The variation of the laser energy deposition in the overcritical region ($10n_c$) and in the critical region are also plotted in Figure 3. For very steep gradients, most of the energy is absorbed in the dense plasma region. However, for gradient scale lengths larger than $5nm$, more than 50% of laser energy is absorbed at critical or near critical density. This shows that resonance absorption becomes the dominant laser absorption mechanism for large scale lengths, leading to a complete disappearance of the surface wave.

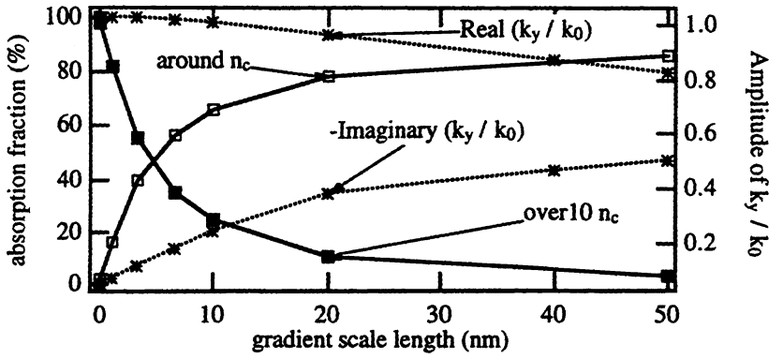

Figure 3: Surface wave vector and localization of the absorption as a function of the gradient scale length. Solid line: absorption fraction in overcritical ($10n_c$) and critical regions. Dashed lines: real and imaginary parts of k_y.

2.3 How to couple a plane wave to a surface wave ?

We have seen in Figure 1 that the dispersion relation of a plane wave incident at an angle θ from the target normal never intersects the dispersion curve of surface waves. Two different ways of coupling the incident wave to a surface wave have been proposed. First, it is possible to modify the dispersion curve of the surface wave by altering the electron density profile in front of the target. This was put forward, in the seventies, to interpret CO_2 laser interaction experiments.[34] Second, we have seen before that it is possible to use a diffraction grating as a target. The groove spacing d of the grating has to be correctly chosen to realize the "phase matching" condition ($k_g = 2\pi/d$; $k_y = k_g + k_0 cos\theta$). In that case, the plane incident wave can be diffracted by the grating into surface modes. Diffraction efficiency is governed by the properties of the grating profile.[25] Without dissipation, the amplitude of a surface wave excited by a constant amplitude plane wave increases secularly as it propagates along the surface. This resonant behavior is similar to the one found in standard resonance absorption.[24] Damping mechanisms usually limit the growth rate of the resonance. They are: i) the ordinary dissipation term related to the imaginary part of the dielectric constant and ii) the diffraction of the surface wave itself on the grating, resulting in radiative modes (radiative decay). Accordingly, similar to resonance absorption for $L^* \approx 1$, laser enery absorption is expected to be important by coupling to surface waves. Assuming that the dispersion relation of

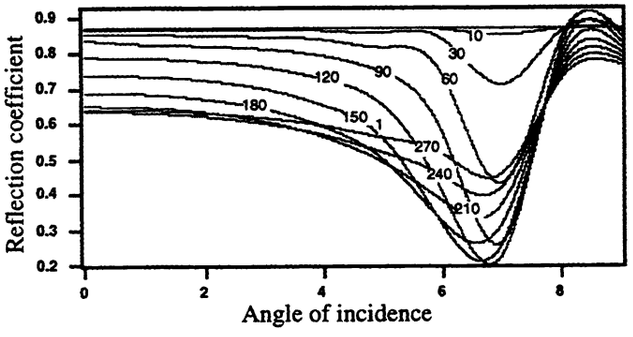

Figure 4: Reflection coefficient as a function of the angle of incidence in the case of a steep gradient. Curves are labeled according to the groove depth in nm. $\lambda = 1000nm$, groove spacing $890nm$.

surface waves is not perturbed too much by the surface corrugation, diffraction orders (evaluated from the "phase matching" conditions) are easily calculated using the standard grating equation: $k_0 \sin\theta' = k_0 \sin\theta + nk_g$ where θ and θ' are the incident and diffracted angles, respectively and n is the diffraction order. The calculation of the

absorption by the grating is more complicated. It can be interpreted as the coupling between several phenomena: collisional damping, interferences between the incident wave, the surface wave (and its own diffraction by the grating), the diffracted waves, and so on. To calculate the absorption coefficient, or equivalently the grating diffraction efficiency, one has to solve the Maxwell equations taking into account the geometry of the interface.

Numerical models have been developed for the optimization of diffraction by the use of multilayer coatings.[25] We have used such a code to calculate the absorption of a plasma in front of a grating. The local dielectric constant was estimated as a function of density and collisionality by using the Drude model. Figure 4 gives the results of such calculations for a steep electron density gradient as a function of the angle of incidence. We have plotted the reflection coefficient for different groove depths for a sinusoidal grating of $890nm$ groove spacing and $1000nm$ laser wavelength. On can see the absorption peak at an angle of $\approx 7°$ corresponding to this particular grating parameters. The position of the resonance depends only slightly on the groove depth. This confirms our assumption that the dispersion relation of surface waves on a grating is only slightly modified from its flat target value. As we have mentioned previously, we also note that the broadening of the resonance is related to the radiative decay time of the surface wave: the deeper the grating grooves, the larger the resonance width.

2.4 Transition between surface wave absorption and grating-modified resonance absorption

We have also studied finite scale length exponential gradients. To do that, we have used a series of 16 plasma layers in our model. The dielectric constant of each layer was given by the Drude model approximation. Resonance absorption at critical density was modeled by using a special layer which thickness dl was related to the wave breaking effective collision rate ν by the usual relation $dl = L\nu/\omega$. We have tested the validity of our calculation model by first obtaining some results on a flat target. In such a case, we should recover the standard results of resonance absorption.[24] Results of our calculations are given in Figure 5a. We find a good qualitative agreement, both in incidence angle position and absorption fraction, between our crude model and more involved calculations.[16,17] In particular, the fact that the absorption maximum is displaced towards grazing angles for steep electron density gradients is in accord with more elaborate calculations of resonance absorption.[15,16]

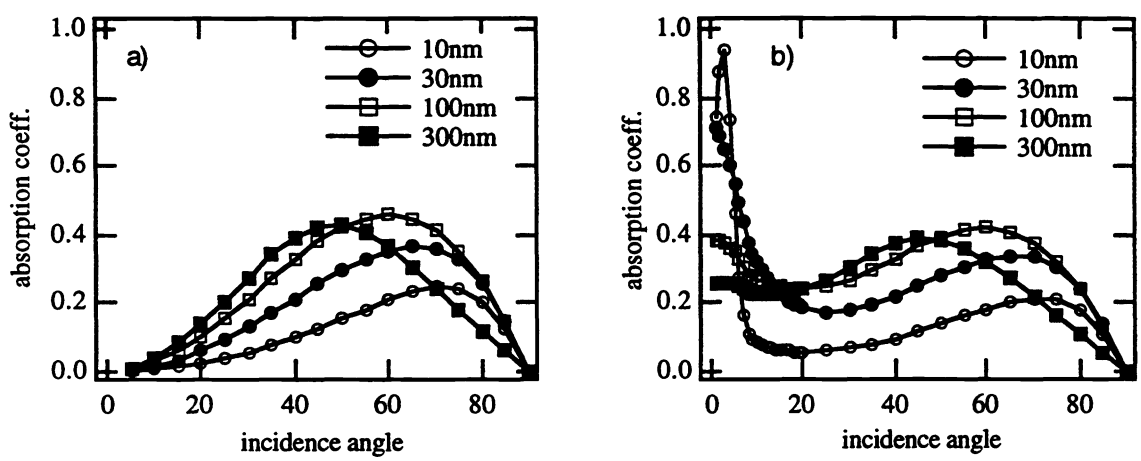

Figure 5: Absorption fraction as a function of the angle of incidence on a) flat target and b) grating, as a function of the gradient scale length in nm. $\lambda = 1000nm$, groove spacing $890nm$, groove depth $100nm$.

In Figure 5b, we have plotted the absorption coefficient calculated for a $100nm$ depth grating and with characteristics similar to the one used in Figure 4. A sharp peak is observed close to the resonance angle for the $10nm$ gradient scale length. When we increase the scale length, we recover the results of Figure 3 where we showed the strong damping of the surface wave for scale lengths in excess of $30nm$. However, a larger absorption

is observed below 20° in the case of the grating compared to the case of the flat target. This can be easily explained because, even near normal incidence, there is always a component of the incident electric field parallel to the local electron density gradient. We have studied this specific effect by using a grating with a groove spacing equal to the laser wavelength and a constant gradient scale length of $300nm$. Under these conditions, we have shown previously that the surface wave was completely damped (see Fig.3). Figure 6 gives the results of the absorption coefficient as a function of the grating groove depth between 0 and $300nm$. Starting from the standard results obtained for a flat target, we see a strong increase of the absorption near normal incidence when we increase the groove depth. For small depths below $200nm$, these results can be interpreted qualitatively by considering the variation of the local angle of incidence for all the positions along the grating. Surprisingly, we find a stronger increase of the absorption for larger depths. This can be explained by the existence of localized electromagnetic modes when the groove depth is comparable to the gradient scale length. Then, the deep grating acts as a waveguide with strong losses. We note that our results are in excellent qualitative agreement with recent experimental data obtained by one of us (RWF and his coworkers) in a study of the variations of the reflectivity of a grating target as a function of the groove depth.[23]

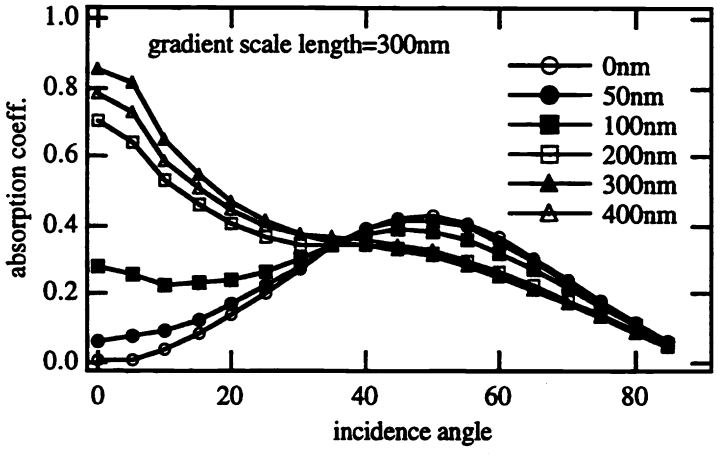

Figure 6: Absorption coefficient as a function of incidence angle for a wavelength equals to the groove spacing ($1000nm$). The gradient scale length is $300nm$. The grating groove depth is varied between 0 and $400nm$.

3 EXPERIMENTAL RESULTS

A Titane:Sapphire laser ($\lambda \approx 800nm$) delivering $120fs$ duration, $50mJ$ energy, $10Hz$ repetition rate laser pulses was focused at intensities ranging from 10^{16} to $10^{17}W/cm^2$ onto silicon flat targets and square-profile gratings. The laser was equipped with a specially designed doublet stretcher[35] to compensate for phase errors of third and fourth order. The laser intensity contrast ratio was better than 10^{-6}. Silicon gratings of $1600nm$ period and $250nm$ groove depth were used. Time-integrated K-shell and $K\alpha$ emissions were dispersed by a Von Hamos spectrograph[8,9] and detected with a cooled (−40°C) x-ray sensitive charge-coupled-device (CCD) camera operating in the single photon counting mode. It was set at an angle of 30° ± 3° from the target normal.

3.1 X-ray spectra on flat targets

Spectra were integrated over a series of 50 shots. The targets were mounted on a carefully aligned X-Y translational stage in order to expose a fresh surface to each laser shot. The size of the CCD matrix being $10mm$, four successive translations of the camera were necessary to record a complete spectrum. Figure 7a shows the spectrum obtained on a flat silicon target for a laser pulse duration of $120fs$. Figure 7b shows another spectrum

obtained under exactly the same conditions but with a laser pulse duration of $1.5ps$ obtained by slightly detuning the grating pair of the compressor stage of the laser system. On both spectra, the spectral range covers the wavelength region between the $1s^2 - 1s2p$ line of He-like silicon to the "cold" $K\alpha$ line.[8] For the longer pulse duration, the lines are fairly narrow, indicative of an electron density significantly lower than solid density. We note the absence of the He-like intercombination line at $6.65\AA$; this is the signature of a plasma with electron densities above critical density ($n_e = 1.6 \times 10^{21} cm^{-3}$). We have studied the qualitative change of the shape of this spectrum with the laser incidence angle. No significant change wad noticed over our experimental range ($10° - 75°$).

The spectrum obtained with a pulse duration of $120fs$ is surprisingly different. Satellite lines from L-like to Bo-like are more intense than the He-like resonance line. Only very small residual structures can be seen on the Li-like satellites around $6.73\AA$. The differences between these two spectra can be qualitatively explained by taking into account the strong variations of the electron density gradient scale length with the pulse duration. We note again that these spectra were obtained with a fairly good laser intensity contrast ratio.

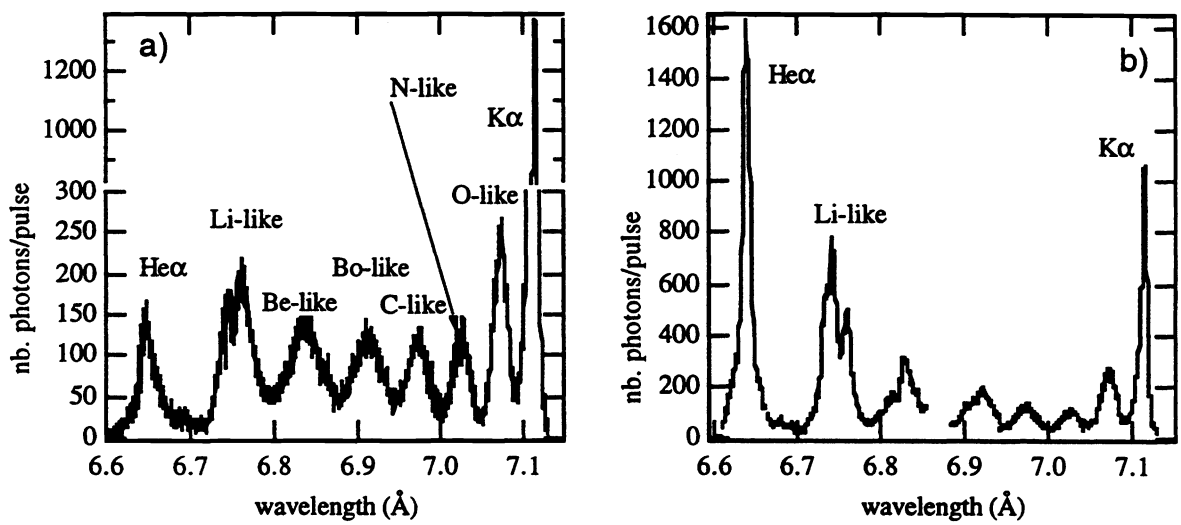

Figure 7: Silicon spectra on flat targets. a) laser pulse duration of $120fs$, b) laser pulse duration of $1.5ps$. Laser irradiance is $5 \times 10^{16} W/cm^2$.

With the shorter pulse duration, the laser interacts directly with the solid target and we observe a spectrum which is characteristic of a high density plasma ($\geq 10^{23} cm^{-3}$). However, ionic populations are out of equilibrium and suprathermal electrons originating from non linear mechanisms like resonance absorption play an important role in the formation of the satellite spectra.[8,36] For longer pulse durations, the electron density gradient scale length increases and the spatial region where He-like and satellite emission occurs is shifted towards lower, but still overcritical, electron densities.

3.2 X-ray spectra as a function of the incidence angle

The He-like resonance line intensity was studied as a function of the incidence angle on flat target and on the grating targets. We used p-polarized light (TM polarization) and the plane of incidence was perpendicular to the grating grooves. Figure 8 shows the results. X-ray emission is practically independent on the incidence angle on flat targets. The small increase of laser absorption with incidence angle for short gradient scale lengths ($0.001 < L^* < 0.01$) is overcompensated by the variations of the laser spot surface over which laser energy deposition occurs.[17] With the grating, X-ray emission shows a maximum for an angle of $35° - 40°$ in good agreement with the dispersion properties of the grating that we have used. Indeed, the groove spacing is twice

the laser wavelength which, taking into account the finite conductivity of the grating material, gives an optimum angle of 35°.

We have done a similar series of experiments looking to the $K\alpha$ line around 7.1$\AA$. Results are given in Figure 9. The shape of the emission as a function of the incidence angle in the case of a grating target is much broader than in the case of the flat target (see Figure 8). With a flat target, the increase of the x-ray intensity as a function of the incidence angle is explained by the increase of the laser wave coupling with the longitudinal volume plasma waves. Indeed, the conversion efficiency into $K\alpha$ radiation depends directly on the laser energy conversion into suprathermal electrons. The theoretical study of the competition between surface wave absorption and resonance absorption resulting in highly energetic electrons is actually in progress. The steady-state model described in

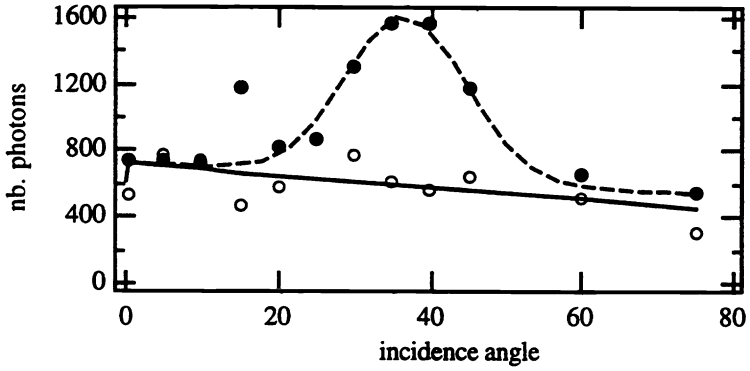

Figure 8: He-like resonance line intensity as a function of the angle of incidence on the grating (dots) and on the flat target (circles). Curves are visual aids to the eye.

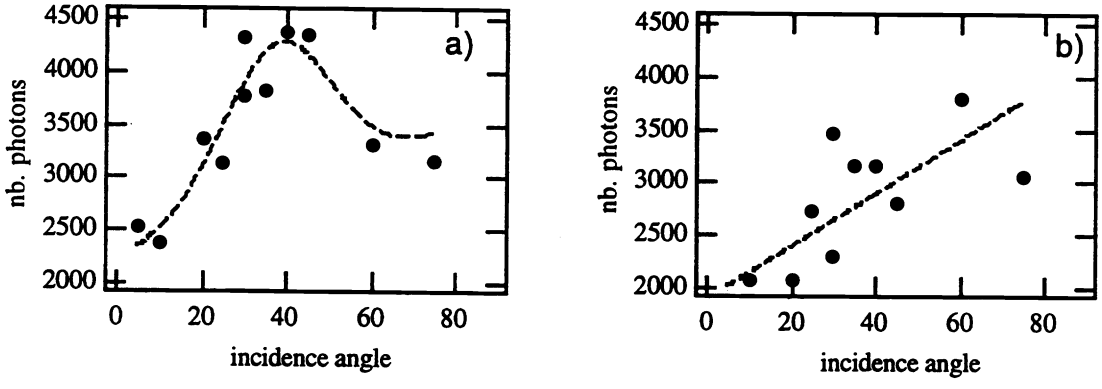

Figure 9: $K\alpha$ resonance line intensity as a function of the angle of incidence on the grating a) and on the flat target b). Curves are visual aids to the eye.

Section 2 has been used to try to explain the shape of x-ray emission with incidence angle in the case of the "thermal" emission of the He-like resonance line. Figure 10 shows the absorption coefficient calculated with this model as a function of incidence angle for a flat and a grating target using the parameters of the experiment. We note that our calculations were performed with a sinusoidal grating shape while the experiment were done with a square grating shape. In addition, our calculations do not take into account the finite size of the focal spot which strongly limit the number of grooves which participate in the diffraction process. We find a good agreement for the angle of maximum emission. For a $10nm$ scale length, the results show the very slight increase of absorption with the angle which is overcompensated by the variations of the deposition energy surface as shown previously in Fig.8. For $30nm$ gradient scale length, the resonant behavior of the grating is completely lost and we recover the standard regime of resonance absorption.

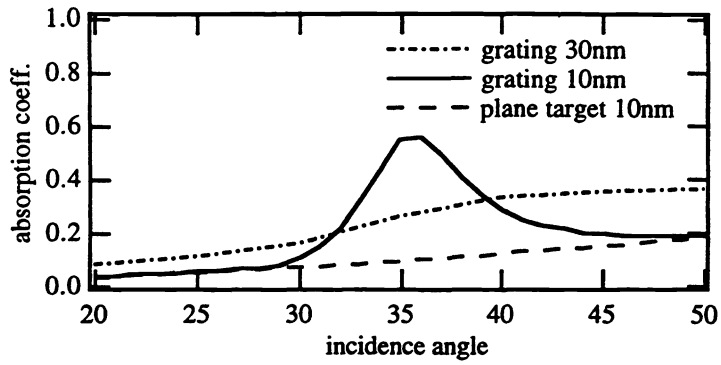

Figure 10: Absorption coefficient of the grating (solid line) and of the flat target (dashed line), both with a $10nm$ gradient scale length, calculated as a function of the angle of incidence with our steady state model. The dashed-dotted curve is for a grating target with $30nm$ gradient scale length.

4 CONCLUSION

We have studied efficient x-ray production above 1 keV using femtosecond laser-produced plasmas on periodically modulated surface targets. Absorption of laser light through the coupling to surface waves has been studied theoretically using a steady-state differential numerical method. A transition between surface wave absorption for steep electron density gradients and resonance absorption for long scale length gradients has been evidenced numerically. Silicon gratings of $1600nm$ period and $250nm$ groove depth were irradiated by a $120fs$, $25mJ$ Ti:sapphire laser ($\lambda \approx 800nm$) at intensities in excess of $10^{16}W/cm^2$. He-like and Li-like satellites spectra of silicon have been recorded for two laser pulse durations. For long pulses ($1.5ps$), the spectral shape of these transitions is similar to the one obtained previously[8,21] with flat targets and an optimized ASE prepulse. For short pulses ($120fs$) and good laser intensity contrast (10^{-6}), the spectral width of these transitions is surprisingly large, indicating electron densities well in excess of $10^{23}cm^{-3}$. A more detailed analysis of spectral line formation under these conditions is underway. X-ray intensities around 1.85 keV (K-shell lines) have been measured as a function of the incidence angle. X-ray conversion efficiencies 2 times larger than those obtained on flat silicon targets have been measured at the "phase matching" angle of our particular grating. The conversion efficiency to $K\alpha$ transitions measured on flat targets was found to increase with the incidence angle, reaching at grazing incidence ($\theta > 70°$) the values obtained with the grating targets at the optimum angle of incidence (35°). Collimated second harmonic generation at definite angles (given by the grating "phase matching" conditions) has also been observed. Two dimensional particle-in-cell simulations are underway to study, in a fully time and space dependent manner, the effects of resonant surface electromagnetic waves on laser absorption and the strong increase of local fields near the corrugated surface. Experimentally, we plan to repeat these measurements with better optimized gratings.

5 ACKNOWLEDGMENTS

We greatly acknowledge the help of the technical staff at the Laboratoire d'Optique Appliquée. We thank G. Granet for the use of his numerical code. This work was supported by the Centre National de la Recherche Scientifique and by an EU Human Capital and Mobility program.

6 REFERENCES

[1] M. M. Murnane, H. C. Kaypten, M. D. Rosen, and R. W. Falcone, "Ultrafast X-ray pulses from laser-produced plasmas," Science **251**, 531 (1991).

[2] U. Teubner, J. Bergmann, B. van Wonterghem, F. P. Schäfer, and R. Sauerbrey, "Angle-dependent x-ray emission and resonance absorption in a laser-produced plasma generated by a high intensity ultrashort pulse," Phys. Rev. Lett. **70**, 794 (1993).

[3] A. Mens, R. Sauneuf, P. Schirman, R. Verrecchia, P. Audebert, J.-C. Gauthier, J.-P. Geindre, A. Antonetti, J.-P. Chambaret, G. Hamoniaux, and A. Mysyrowicz, "The C850X ultrafast streak camera: an instrument to study spatially and temporally subpicosecond laser-matter interaction," *UltraFast Phenomena VIII,* eds. J.L Martin, A. Migus, G. Mourou, A. Zewail (Springer-Verlag, 1992), Vol. 55, p. 147.

[4] H. M. Milchberg, R. R. Freeman, and S. C. Davey, "Resistivity of a simple metal from room temperature to $10^6 K$," Phys. Rev. Lett. **61**, 2364 (1988).

[5] M. M. Murnane, H. C. Kaypten, and R. W. Falcone, "Studies of hot dense plasmas produced by an intense subpicosecond laser," Phys. Rev. Lett. **62**, 155 (1989).

[6] J. C. Kieffer, M. Chaker, J. P. Matte, H. Pépin, Y. Coté, Y. Beaudoin, T. W. Johnston, C. Y. Chien, S. Coe, G. Mourou, and O. Peyrusse, "Ultra fast X-ray sources," Phys. Fluids, **B5**, 2330 (1993).

[7] M. D. Rosen, "Scaling laws for femtosecond laser-plasma interactions," Proc. SPIE **1229**, 60 (1990).

[8] R. Mancini, P. Audebert, J.P. Geindre, A. Rousse, F. Falliès, J.-C. Gauthier, A. Mysyrowicz, J.P. Chambaret and A. Antonetti, "The formation of Li-like satellites during the interaction of femtosecond laser pulses with Al targets," J.Phys. B: At. Mol. Opt. Phys. **27**, 1671, (1994).

[9] P. Audebert, J.-P. Geindre, A. Rousse, F. Falliès, J.-C. Gauthier, A. Mysyrowicz, J.-P. Chambaret, and A. Antonetti, "K-shell emission dynamics of Be-like to He-like ions from a 100fs laser-produced aluminium plasma," J. Phys. B: Atom. Optical Mol. Phys. **27**, 3303 (1994).

[10] A. Rousse, P. Audebert, J.-P. Geindre, F. Falliès, J.-C. Gauthier, A. Mysyrowicz, G. Grillon, and A. Antonetti, "Efficient Kα X-ray source from femtosecond laser-produced plasmas," Phys. Rev. **E50**, 2200 (1994).

[11] A. Rousse P. Audebert, J. P. Geindre, F. Falliès, J.-C. Gauthier, A. Mysyrowicz, G. Grillon and A. Antonetti, "Observation of x-ray fluorescence resulting from photoionization by a femtosecond laser-produced plasma x-ray source," J. Phys. B: Atom. Optical Mol. Phys. **27**, L697 (1994).

[12] H. M. Milchberg, I. Lyubomirsky, and C. G. Durfee. III, "Factors controlling the x-ray pulse emission from an intense femtosecond laser heated solid," Phys. Rev. Lett. **67**, 2654 (1991).

[13] D. D. Meyerhofer, H. Chen, J. A. Delettrez, B. Soom, S. Uchida, and B. Yaakobi, "Resonance absorption in high-intensity contrast picosecond laser-plasma interactions," Physics Fluids, **B5**, 2584 (1993).

[14] H. Chen, B. Soon, B. Yaakobi, S. Uchida, and D. D. Meyerhofer, "Hot electron characterization from $K\alpha$ measurements in high-contrast p-polarized picosecond laser-plasma interaction," Phys. Rev. Letters, **70**, 3431 (1993).

[15] H. M. Milchberg, and R. R. Freeman, "Light absorption in ultrashort scale length plasmas," Jl. Opt. Soc. Amer. B **6**, 1351 (1989).

[16] R. Fedosejevs, R. Ottmann, R. Sigel, G. Kühnle, S. Szatmari, and F. P. Schäfer, "Absorption of subpicosecond ultraviolet laser pulses in high-density plasma," Appl. Phys. B **50**, 79 (1990); R. Fedosejevs, R. Ottmann, R. Sigel, G. Kühnle, S. Szatmari, and F. P. Schäfer, "Absorption of femtosecond laser pulses in high-density plasma," Phys. Rev. Lett. **64**, 1250 (1990).

[17] F. Falliès, "Etude numérique et expérimentale de l'interaction d'une impulsion laser subpicoseconde avec une cible solide," Thèse de l'Université Paris-6, Paris (1994).

[18] U. Teubner, C. Wülker, W. Theobald, and E. Förster, "X-ray spectra from high-intensity subpicosecond laser-produced plasmas," Phys. Plasmas, **2**, 972 (1995).

[19] J. C. Kieffer, M. Chaker, Y. Coté, Y. Beaudoin, H. Pépin, C. Y. Chien, S. Coe, and G. Mourou, "Ultrafast x-ray emission from ultrashort plasmas," Appl. Optics **32**, 4247 (1993).

[20] C. Wülker, W. Theobald, F. P. Schäfer, and J.S. Bakos, "Temporal behavior of x-ray radiation emitted by subpicosecond KrF-laser-heated carbon preplasmas", Phys. Rev. **E50**, 4920 (1994).

[21] J.-C. Gauthier, A. Rousse, F. Falliès, J.-P. Geindre, P. Audebert, A. Mysyrowicz, G. Grillon, J.-P. Chambaret, and A. Antonetti, "Influence of the prepulse on the x-ray yield of a subpicosecond laser-produced plasma," in "Laser Interactions with Atoms, Solids and Plasmas", ed. R.M. More, NATO ASI Series B: Physics, Vol. **237**, (Plenum, New York, 1994), p. 357.

[22] V. N. Seminogov, and A. I. Khudobenko, "Non-linear generation of the fundamental and first harmonic of a periodic surface profile under the action of s-polarized laser radiation," Sov. Phys. JETP, **69**, 284 (1989).

[23] M. M. Murnane, H. C. Kaypten, S. P. Gordon, J. Bokor, E. N. Glytis, and R. W. Falcone, "Efficient coupling of high intensity subpicosecond laser pulses into solids," Appl. Phys. Lett. **62**, 1068 (1993).

[24] W.L. Kruer, *The Physics of Laser Plasma Interaction* (Addison-Wesley, Redwood City, 1988), Chap. 4, p. 37.

[25] J. Chaudezon, M. T. Dupuis, G. Cornet, and D. Maystre, "Multicoated gratings: a differential formalism applicable in the entire optical region," J. Opt. Soc. Am. **72**, 839 (1982).

[26] H. Raether, *Surface Plasmons*, Springer Tracts in Modern Physics, (Springer, 1988), Vol. 11.

[27] M. C. Hutley, and D. Maystre, "The total absorption of light by a metallic grating," Optics Comm. **19**, 431 (1976).

[28] D. Maystre, and R. Petit, "Brewster incidence for metallic gratings," Optics Comm. **17**, 196 (1976).

[29] D. J. Ehrlich, S. R. J. Brueck, and J. Y. Tsao, "Time resolved measurements of stimulated surface polariton waves scattering and grating formation in pulsed laser annealed germanium," Appl. Phys. Lett. **41**, 630, (1982).

[30] V. I. Emelyanov, E. M. Zemskow, and V. N. Seminogov, "Theory of formation of surface gratings under the action of laser radiation on surfaces of metals, semiconductors and insulators," Sov. J. Quant. Elec. **13**, 1556, (1983).

[31] M. I. Tribelskii, and S. M. Gold'berg, "Resonant excitation of electromagnetic surface waves in laser evaporation of condensed media," Sov. Tech. Phys. Lett. **8**, 526, (1982).

[32] A. Septier, "Renforcement du rendement des photocathodes métalliques par excitation d'ondes de surface," Rapport PMI 2586, (1992). Available upon request to the authors.

[33] J.C. Dudeck, "L'effet de peau anormal dans les metaux nobles. Impédance de surface et modélisation des couches minces polycristallines," Rapport de synthèse CNAM (1989). Available upon request to the authors.

[34] Hiroatsu Maki, and Keishiro Niu, "High absorption of laser light in target plasma with plateau-ramp-type density profile," J. Phys. Soc. Japan **45**, 269 (1978).

[35] A. Sullivan, and W. E. White, "Phase control for production of high-fidelity optical pulses for chirped-pulse amplification," Opt. Letters **20**, 192 (1995).

[36] O. Peyrusse, J. C. Kieffer, C. Y. Coté, and M. Chaker, "$1s2l2l' - 1s^2 2l$ line spectra in high density, non-Maxwellian and highly transient plasmas," J. Phys. B: At. Mol. Opt. Phys. **26**, L511 (1993).